Spin-liquid signatures in the quantum critical regime of pressurized CePdAl

M. Majumder,[1,2] R. Gupta,[3] H. Luetkens [ID],[3] R. Khasanov,[3] O. Stockert [ID],[4] P. Gegenwart [ID],[2] and V. Fritsch [ID][2]

[1]*Department of Physics, Shiv Nadar University, Gautam Buddha Nagar, Uttar Pradesh 201314, India*
[2]*Experimental Physics VI, Center for Electronic Correlations and Magnetism, University of Augsburg, 86159 Augsburg, Germany*
[3]*Laboratory for Muon Spin Spectroscopy, Paul Scherrer Institut, 5232 Villigen PSI, Switzerland*
[4]*Max Planck Institute for Chemical Physics of Solids, 01187 Dresden, Germany*

CePdAl is a prototypical frustrated Kondo lattice with partial long-range order (LRO) at $T_N = 2.7$ K. Previous bulk experiments under hydrostatic pressure found signatures for a quantum critical regime that extends from $p_c \approx 0.9$ GPa, where LRO disappears, up to ~ 1.7 GPa. We employed extensive muon spin relaxation and rotation experiments under pressure. The continuous and complete suppression of LRO at p_c is confirmed. Above $T_N(p)$ and beyond p_c, an additional crossover scale $T^*(p)$ characterizes the change from pure to stretched exponential relaxation in zero field. Remarkably, $T^*(p)$ agrees with previously determined signatures of entropy accumulation above LRO. This coincidence microscopically evidences fluctuating frustrated spins at $T \leqslant T^*$ with spin-liquid behavior. Power-law divergences of the temperature and longitudinal field dependences of the relaxation rate, with time-field scaling, at pressures between p_c and 1.7 GPa characterize this regime as quantum critical.

Introduction. Due to the presence of competing interactions, strongly correlated electron systems react inherently susceptible to chemical composition or the application of pressure. The tuning of such nonthermal parameters often induces a quantum critical point (QCP), where magnetic order is continuously suppressed to zero temperature. Experimentally, non-Fermi-liquid behavior was detected in the last decades for numerous quantum critical materials, most notably in the class of heavy-fermion metals, where it arises from the competition between the Kondo effect and the indirect exchange interaction between the $4f$ electrons [1]. Its theoretical description is particularly challenging if a divergence of the quasiparticle mass indicates a severe failure of Fermi-liquid theory, beyond the framework of spin-density-wave criticality [2]. Advanced scenarios such as Fermi-liquid fractionalization [3], breakdown of Kondo entanglement [4], or strong-coupling critical Fermi liquid [5] were proposed. Within a "global phase diagram" unconventional quantum criticality as well as a metallic spin-liquid state with localized $4f$ moments was proposed to arise from strong quantum fluctuations, induced by low-dimensional and frustrated magnetic couplings [6–8]. An experimental investigation of quantum criticality in frustrated Kondo lattices is therefore of particular interest.

The hexagonal ZrNiAl structure features equilateral triangles of Zr atoms, forming a distorted kagome lattice, offering the possibility of frustration when $4f$ moments are placed on the Zr lattice sites. For example, in YbAgGe, as a function of applied magnetic field, a series of almost degenerate magnetically ordered states arises below 1 K with a quantum bicritical metamagnetic endpoint and pronounced non-Fermi-liquid behavior in its vicinity [9,10]. While in YbAgGe the $4f$ electrons are well localized due to a very weak Kondo interaction, isostructural CeRhSn and CeIrSn are Kondo lattices within the intermediate valence regime [11,12]. For CeRhSn zero-field quantum criticality was detected, which is tunable by in-plane uniaxial pressure and related to geometrical frustration [13,14]. CeIrSn features even stronger valence fluctuations, as recently confirmed spectroscopically [12]. Despite a huge $T_K \approx 480$ K, emergent antiferromagnetic (AFM) correlations where detected below 1 K, suggesting that strong frustration counteracts Kondo singlet formation even in the intermediate valence regime [12].

We focus on isostructural CePdAl with $T_K \approx 5$ K [15] which stands out of the class of geometrically frustrated Kondo systems due to its unique coexistence of AFM order below $T_N = 2.7$ K [16] with magnetic frustration, evidenced by the fact that one of three Ce moments in the crystallographic unit cell remains fluctuating down to 30 mK [17,18]. Powder neutron diffraction was described by a simplified model. Within the basal plane, ferromagnetic (FM) nearest-neighbor interactions compete with next-nearest-neighbor AFM coupling, leaving Ising spins (along the c axis) that form FM chains of Ce(1) and Ce(3) atoms, separated by fluctuating Ce(2) moments [17]. A detailed magnetic and thermodynamic investigation on single-crystalline CePdAl under c-axis magnetic field found a scale $T_S(B)$, where magnetization $M(T)$ and entropy $S(B)$ display maxima [19]. In the absence of frustration, such entropy accumulation should occur at the AFM
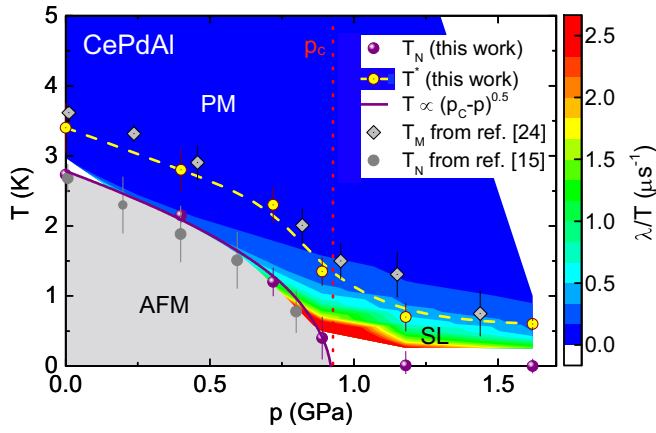
FIG. 1. Temperature-pressure magnetic phase diagram of CePdAl combined with a contour plot of the pressure- and temperature-dependent relaxation rate $\lambda(p, T)$ in CePdAl, plotted as $\lambda(p, T)/T$. Apart from the antiferromagnetically ordered (AFM) and the paramagnetic (PM) phases there exists an extended region around and above pressure-induced quantum criticality (at p_c) with spin-liquid (SL) properties. The Néel temperatures T_N extracted from weak transverse-field μSR (purple symbols, error bars indicate the width of the transition) agree well with reported values (gray symbols) from susceptibility measurements [15]. Open circles and open squares display $T^*(p)$ and the entropy accumulation line $T_S(p)$ (see Ref. [24], therein labeled as T_M), respectively. The solid line corresponds to $(p_c - p)^{0.5}$ with $p_c = 0.92$ GPa while the dashed line is a guide to the eye.

phase boundary, while for CePdAl it arises significantly above $T_N(B)$, indicating a regime with spin-liquid behavior at $T_N \leqslant T \leqslant T_S$ [19]. The AFM order in CePdAl can be continuously suppressed by chemical substitution in the alloying series CePd$_{1-x}$Ni$_x$Al [20–22]. Thermodynamic evidence for quantum criticality was found and an additional entropy signature beyond the QCP arises, likely related to persistent correlations of the frustrated Ce(2) moments [21]. The AFM order can also be suppressed by hydrostatic pressure [15,23,24], yielding a QCP at $p_c \approx 0.9$ GPa. Maxima in the temperature dependence of the ac susceptibility were used to determine $T_S(p)$; interestingly, it persists beyond the critical pressure up to about 1.7 GPa and was interpreted as a paramagnetic phase with $4f$ electrons that neither order nor form a Fermi liquid [24–26].

In this Letter, we report detailed low-temperature muon spin relaxation/rotation (μSR) measurements under hydrostatic pressure performed at the muon source of the Paul Scherrer Institute in Switzerland which provide microscopic evidence for a quantum critical regime with spin-liquid properties in CePdAl. All relevant details on samples, spectrometers, and data analysis can be found in the Supplemental Material [27].

Nature of ordered state under pressure. Weak transverse-field (wTF) measurements were performed to follow the Néel temperature T_N as a function of pressure p [27]. As displayed in Fig. 1, $T_N(p)$ agrees well with bulk measurements [15] and is suppressed in a mean-field-like behavior, i.e., $T_N(p) \propto (p_c - p)^{0.5}$ with $p_c = 0.92$ GPa. Figures 2(a) and 2(b) show selected zero-field (ZF) μSR spectra for ambient and various applied pressures. The ambient pressure spectrum at 1.58 K,
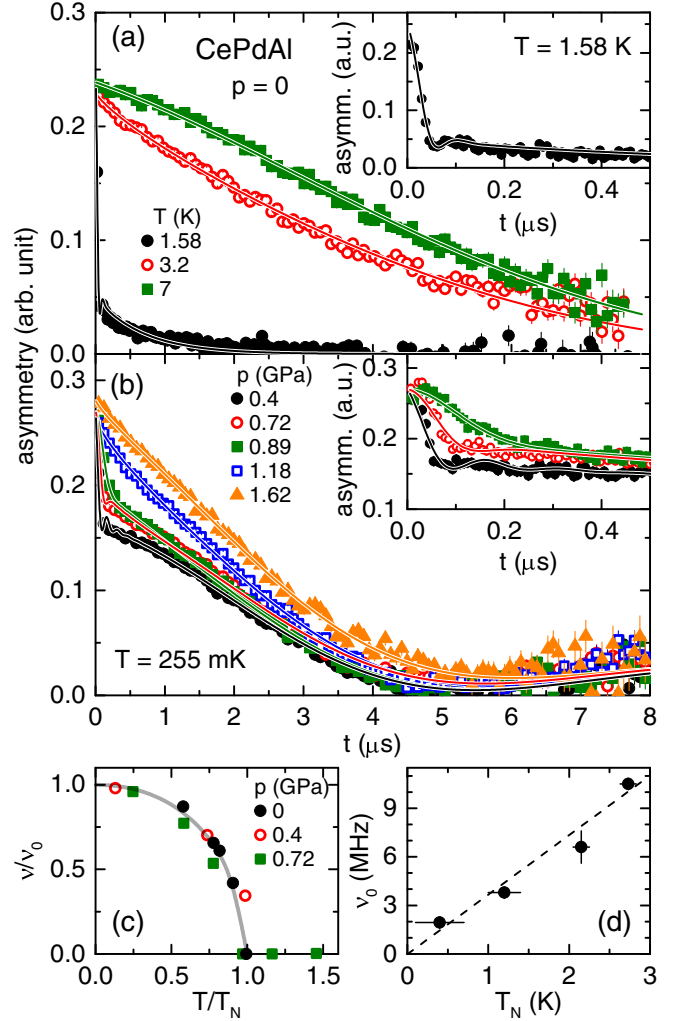

FIG. 2. Zero-field (ZF) asymmetry spectra in CePdAl (a) for different temperatures at ambient pressure and (b) at 255 mK for different hydrostatic pressures. Insets in (a) and (b) zoom into the initial relaxation at early times. (c) Normalized muon oscillation frequency ν/ν_0 [$\nu_0 = \nu(T = 0)$] vs normalized temperature T/T_N for different pressures. (d) Muon oscillation frequency ν_0 vs ordering temperature T_N indicating a linear dependence (dashed straight line). Solid lines denote fits to the data (for details, see text).

i.e., below T_N, contains a highly damped oscillating component [cf. inset of Fig. 2(a)], that is absent in the paramagnetic state, in addition to the background relaxation. The best fit to the zero-field μSR spectra is obtained using

$$A(t) = A_0 \left[f_{\text{sample}} \left\{ \frac{2}{3} j_0 \left(2\pi \nu t + \frac{\pi \phi}{180} \right) e^{-\frac{(\sigma t)^2}{2}} + \frac{1}{3} e^{-\lambda_L t} \right\} \right.$$
$$\left. + (1 - f_{\text{sample}}) e^{-\lambda_{\text{Bkg}} t} \right]. \quad (1)$$

Here, A_0 is the initial asymmetry and σ the muon transverse depolarization rate (arising from a distribution of internal fields) forming a Gaussian envelope to the oscillating component with a frequency ν and phase ϕ (set to zero in our case). Furthermore, λ_L is the longitudinal relaxation rate, f_{sample} the fraction of moments taking part in the long-range

order (LRO), and λ_{Bkg} the relaxation rate of the background contribution. At 1.5 K, $f_{\mathrm{sample}} \approx 85\%$ which matches with the sample contribution found in wTF measurements. Thus, we kept this fraction fixed below T_N. The need of the Bessel function (j_0) indicates an incommensurate long-range magnetic ordering consistent with neutron scattering and NMR experiments [17,18,28].

Data taken in the pressure cell were analyzed by the same function, taking into account the cell background [27]. At the lowest temperature $T = 255$ mK the oscillation frequency ν of the ZF asymmetry clearly decreases with pressure [cf. Fig. 2(b)] and beyond 0.89 GPa, signs of LRO are no longer found. The normalized temperature dependence of the oscillation frequency for different pressures below p_c, displayed in Fig. 2(c) and representing the order parameter, can be described by $\nu(T) = \nu_0[1 - (T/T_N)^{\alpha'}]^{\beta'}$, following Refs. [29,30], with pressure-independent exponents $\alpha' = 2.2$ and $\beta' = 0.5$ [solid line in Fig. 2(c)]. This suggests a persistent nature of the LRO up to the QCP, together with a continuous decrease of the ordered moment. The linear dependence of the ordered moment, being proportional to the muon oscillation frequency ν_0, on T_N shown in Fig. 2(d), is in line with earlier reports on CePd$_{1-x}$Ni$_x$Al and pressurized CePdAl [22].

Pressure dependence of spin dynamics in the paramagnetic state. The ZF-μSR spectra in the paramagnetic state above $T_N(p)$ are fitted by a static Gaussian Kubo-Toyabe function (for the nuclear moment contribution) multiplied by an exponential function with a stretched exponent β for the dynamics of the electronic moments:

$$A(t) = A_0\left[\left(\frac{1}{3} + \frac{2}{3}\{1 - (\sigma_{\mathrm{nucl}}t)^2\}e^{-\frac{(\sigma_{\mathrm{nucl}}t)^2}{2}}\right)e^{-(\lambda t)^\beta}\right]. \quad (2)$$

We obtain a temperature-independent $\sigma_{\mathrm{nucl}} \simeq 0.1325$ μs^{-1}, while the evolution of the relaxation rate λ and stretching exponent β with temperature and pressure is depicted in Fig. 3. We first discuss the evolution of β. At ambient pressure, a change from purely exponential ($\beta = 1$) to stretched exponential ($\beta < 1$) behavior is found below about 3.5 K. A transition to stretched exponential behavior is characteristic for disordered (fluctuating) moments and is regularly found in spin glasses [31] and frustrated magnets [32,33]. Note that we do not see any indication of static fields from frozen moments at any pressure and temperature in CePdAl. In addition, the stretching exponent is far larger than 1/3, characteristic for a spin glass at the freezing temperature [31]. We therefore associate the stretched exponential behavior at $T \leqslant T^*(p)$ [cf. the arrows in Fig. 3(b)] with the development of spin-liquid-type correlations. In this temperature range, quite strong but very short-range AFM correlations are visible in neutron scattering [22]. Most importantly, $T^*(p)$ agrees very well with the previously determined entropy accumulation $T_S(p)$ from bulk magnetic susceptibility. This provides microscopic evidence for frustrated magnetism over a wide parameter range, enclosing the LRO phase. Further information is contained in the temperature dependence of the relaxation rate $\lambda/T = 1/T_1T \propto \chi''(q,\omega)$, where $\chi''(q,\omega)$ is the imaginary part of the dynamical spin susceptibility. The strong increase of λ/T towards low T, shown for various pressures in Fig. 3(a), thus indicates the (critical) slowing down of the spin fluctuations.
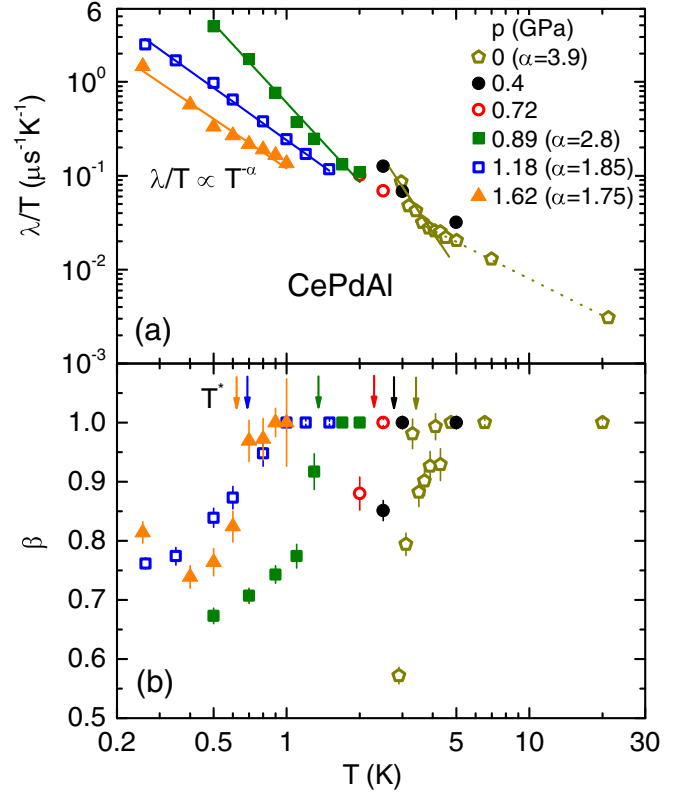

FIG. 3. (a) Temperature dependence of the relaxation rate λ in CePdAl plotted as λ/T in zero field for various pressures. Solid lines represent power-law divergences ($T^{-\alpha}$). (b) Stretching exponent $\beta(T)$ at different pressures. Arrows indicate $T^*(p)$, where β decreases below 1. For details, see text.

At and beyond p_c the divergence holds to lowest measured T, indicative of quantum critical behavior, although we do not observe a universal, i.e., pressure-independent, critical exponent. As visualized in the contour plot (Fig. 1), it is the regime beyond p_c for which this divergence in λ/T vs T is most prominent, providing microscopic evidence of a quantum critical regime with spin-liquid behavior that extends up to at least $1.75p_c$.

Quantum criticality close to p_c and beyond. To characterize quantum critical fluctuations indicated by the divergent relaxation rate, we also performed longitudinal field (LF) μSR measurements. Figure 4(a) shows the LF dependence of λ at several fixed temperatures for three different pressures ranging from approximately p_c to $1.75p_c$. In all cases, a power-law divergence towards zero field is found, similar as recently reported for the nearly ferromagnetic metal YFe$_2$Al$_{10}$, where it was shown to resemble the dynamic structure factor $S(\omega, T)$ at the μSR frequencies [34]. With increasing temperature and pressure the exponent γ in $\lambda \propto H^{-\gamma}$ is only weakly reduced [cf. Fig. 4(a)]. Since μSR probes the Fourier transform of the spin-spin autocorrelation function $q(t) = \langle \mathbf{S}_i(t) \cdot \mathbf{S}_i(0)\rangle$, the nature of $q(t)$ (whether it follows a power-law or stretched exponential dependence) can be unambiguously identified by time-field scaling of the μSR asymmetry. Figure 4(b) shows $A(t/H_{\mathrm{LF}}^\gamma)$ scaling over three decades with
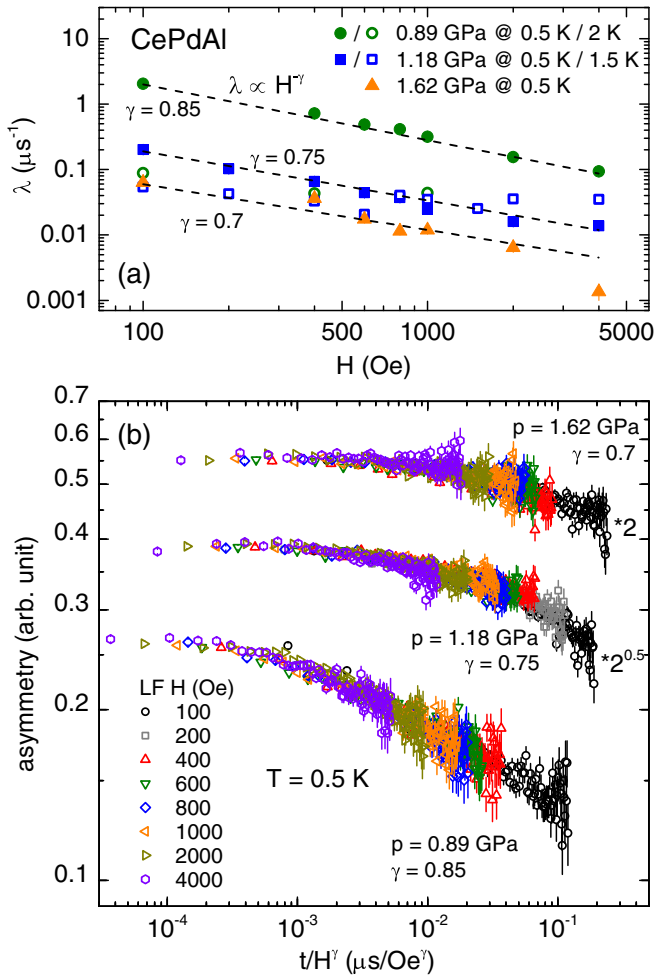
FIG. 4. (a) Longitudinal field dependence of the μSR relaxation rate λ in CePdAl at different pressures and temperatures (dashed lines are fits according to $\lambda \propto H^{-\gamma}$ for $T = 0.5$ K). (b) Time-over-field t/H^{γ} scaling of the asymmetry spectra at 0.5 K for different pressures. The data for different pressures are shifted vertically by a factor $\sqrt{2}$ with respect to each other.

consistent exponents γ for the three pressures. Generally, $\gamma < 1$ signifies a power-law behavior of $q(t)$, unlike $\gamma > 1$ for a stretched exponential behavior in inhomogeneous systems. This strongly indicates that the spin dynamics is cooperative in the "spin-liquid" regime at $p_c \leqslant p < 1.75 p_c$. Furthermore, the LF experiments also signify that the correlations are dynamic, since even at a field of about 2000 Oe no decoupling of the relaxation channels occurs.

Discussion. Generically, quantum criticality shrinks to a narrow control parameter regime at low temperatures. Quantum phase transitions can be smeared by disorder, resulting in a gradual evolution from LRO to a cluster glass with power-law divergences, as observed in CePd$_{1-x}$Rh$_x$ [35]. Extended non-Fermi-liquid regimes have also been observed when the transition changes its nature to first order (discontinuous) near the critical point (cf. e.g., the cases in Sr$_{1-x}$Ca$_x$RuO$_3$ or MnSi under pressure [36,37]). Clear absence of spin freezing, continuous suppression of the order parameter with pressure, and divergence of the relaxation rate upon cooling exclude these scenarios for CePdAl. The onset of stretched exponential relaxation at $T < T^*(p)$ agrees with the entropy accumulation line $T_S(p)$, previously associated with spin-liquid correlations [24]. In this regime, the Ce sites start to become inequivalent as evidenced by neutron diffraction [22]. It is therefore obvious to ask whether the stretched exponential behavior results from the superposition of μSR spectra from different muon stopping sites. However, below $T_N(p)$, the muon stopping site(s) are obviously all sensitive to the static internal field from LRO, since the remaining paramagnetic signal can be associated with the background. This strongly suggests that the stretched exponential relaxation indeed results from dynamical spin-liquid correlations and not from static spin disorder.

Conclusions. Detailed muon spin relaxation and rotation experiments under pressure and down to very low temperatures provide microscopic evidence for a quantum critical point in the hexagonal Kondo lattice CePdAl that is strongly affected by geometrical frustration. An extended regime with spin-liquid behavior is found, with a divergent relaxation rate and quantum critical time over field scaling.

V.F. and O.S. initiated the project and prepared the sample; M.M. suggested and planned the μSR measurements; M.M., R.G., H.L., and R.K. performed the measurements; M.M., R.G., H.L., O.S., P.G., and V.F. discussed the results and analyzed the data; M.M., O.S., and P.G. wrote the manuscript; all authors revised and approved the manuscript.

[1] H. v. Löhneysen, A. Rosch, M. Vojta, and P. Wölfle, Rev. Mod. Phys. **79**, 1015 (2007).

[2] P. Gegenwart, Q. Si, and F. Steglich, Nat. Phys. **4**, 186 (2008).

[3] T. Senthil, S. Sachdev, and M. Vojta, Phys. Rev. Lett. **90**, 216403 (2003).

[4] Q. Si, S. Rabello, K. Ingersent, and J. L. Smith, Nature (London) **413**, 804 (2001).

[5] P. Wölfle, J. Schmalian, and E. Abrahams, Rep. Prog. Phys. **80**, 044501 (2017).

[6] Q. Si, Phys. B: Condens. Matter **378-380**, 23 (2006).

[7] M. Vojta, Phys. Rev. B **78**, 125109 (2008).

[8] P. Coleman and A. H. Nevidomskyy, J. Low. Temp. Phys. **161**, 182 (2010).

[9] J. K. Dong, Y. Tokiwa, S. L. Bud'ko, P. C. Canfield, and P. Gegenwart, Phys. Rev. Lett. **110**, 176402 (2013).

[10] Y. Tokiwa, M. Garst, P. Gegenwart, S. L. Bud'ko, and P. C. Canfield, Phys. Rev. Lett. **111**, 116401 (2013).

[11] Y. Bando, T. Suemitsu, K. Takagi, H. Tokushima, Y. Echizen, K. Katoh, K. Umeo, Y. Maeda, and T. Takabatake, J. Alloys Compd. **313**, 1 (2000).

[12] Y. Shimura, A. Wörl, M. Sundermann, S. Tsuda, D. T. Adroja, A. Bhattacharyya, A. M. Strydom, A. D. Hillier, F. L. Pratt, A. Gloskovskii, A. Severing, T. Onimaru, P. Gegenwart, and T. Takabatake, Phys. Rev. Lett. **126**, 217202 (2021).

[13] Y. Tokiwa, C. Stingl, M.-S. Kim, T. Takabatake, and P. Gegenwart, Sci. Adv. **1**, 1500001 (2015).

[14] R. Küchler, C. Stingl, Y. Tokiwa, M. S. Kim, T. Takabatake, and P. Gegenwart, Phys. Rev. B **96**, 241110(R) (2017).

[15] T. Goto, S. Hane, K. Umeo, T. Takabatake, and Y. Isikawa, J. Phys. Chem. Solids **63**, 1159 (2002).

[16] H. Kitazawa, A. Matsushita, T. Matsumoto, and T. Suzuki, Phys. B: Condens. Matter **199-200**, 28 (1994).

[17] A. Dönni, G. Ehlers, H. Maletta, P. Fischer, H. Kitazawa, and M. Zolliker, J. Phys.: Condens. Matter **8**, 11213 (1996).

[18] A. Oyamada, S. Maegawa, M. Nishiyama, H. Kitazawa, and Y. Isikawa, Phys. Rev. B **77**, 064432 (2008).

[19] S. Lucas, K. Grube, C.-L. Huang, A. Sakai, S. Wunderlich, E. L. Green, J. Wosnitza, V. Fritsch, P. Gegenwart, O. Stockert, and H. v. Löhneysen, Phys. Rev. Lett. **118**, 107204 (2017).

[20] V. Fritsch, N. Bagrets, G. Goll, W. Kittler, M. J. Wolf, K. Grube, C.-L. Huang, and H. v. Löhneysen, Phys. Rev. B **89**, 054416 (2014).

[21] A. Sakai, S. Lucas, P. Gegenwart, O. Stockert, H. v. Löhneysen, and V. Fritsch, Phys. Rev. B **94**, 220405(R) (2016).

[22] Z. Huesges, S. Lucas, S. Wunderlich, F. Yokaichiya, K. Prokes, K. Schmalzl, M.-H. Lemee-Cailleau, B. Pedersen, V. Fritsch, H. v. Löhneysen, and O. Stockert, Phys. Rev. B **96**, 144405 (2017).

[23] K. Prokes, P. Manuel, D. T. Adroja, H. Kitazawa, T. Goto, and Y. Isikawa, J. Magn. Magn. Mater. **310**, e28 (2007).

[24] H. Zhao, J. Zhang, M. Lyu, S. Bachus, Y. Tokiwa, P. Gegenwart, S. Zhang, J. Cheng, Y. Yang, G. Chen, Y. Isikawa, Q. Si, F. Steglich, and P. Sun, Nat. Phys. **15**, 1261 (2019).

[25] J. Zhang, H. Zhao, M. Lv, S. Hu, Y. Isikawa, Y.-F. Yang, Q. Si, F. Steglich, and P. Sun, Phys. Rev. B **97**, 235117 (2018).

[26] J. Wang and Y.-f. Yang, Phys. Rev. B **104**, 165120 (2021).

[27] See Supplemental Material at http://link.aps.org/supplemental/10.1103/PhysRevB.105.L180402 for details on the investigated sample, utilized spectrometers, as well as data analysis, which includes Refs. [38–40].

[28] L. Keller, A. Dönni, H. Kitazawa, and B. van den Brandt, Appl. Phys. A **74**, s686 (2002).

[29] P. J. Baker, I. Franke, F. L. Pratt, T. Lancaster, D. Prabhakaran, W. Hayes, and S. J. Blundell, Phys. Rev. B **84**, 174403 (2011).

[30] S. M. Disseler, C. Dhital, A. Amato, S. R. Giblin, C. de la Cruz, S. D. Wilson, and M. J. Graf, Phys. Rev. B **86**, 014428 (2012).

[31] I. A. Campbell, A. Amato, F. N. Gygax, D. Herlach, A. Schenck, R. Cywinski, and S. H. Kilcoyne, Phys. Rev. Lett. **72**, 1291 (1994).

[32] A. Yaouanc, P. Dalmas de Réotier, Y. Chapuis, C. Marin, G. Lapertot, A. Cervellino, and A. Amato, Phys. Rev. B **77**, 092403 (2008).

[33] Y. Li, D. Adroja, P. K. Biswas, P. J. Baker, Q. Zhang, J. Liu, A. A. Tsirlin, P. Gegenwart, and Q. Zhang, Phys. Rev. Lett. **117**, 097201 (2016).

[34] K. Huang, C. Tan, J. Zhang, Z. Ding, D. E. MacLaughlin, O. O. Bernal, P.-C. Ho, C. Baines, L. S. Wu, M. C. Aronson, and L. Shu, Phys. Rev. B **97**, 155110 (2018).

[35] T. Westerkamp, M. Deppe, R. Küchler, M. Brando, C. Geibel, P. Gegenwart, A. P. Pikul, and F. Steglich, Phys. Rev. Lett. **102**, 206404 (2009).

[36] Y. J. Uemura, T. Goko, I. M. Gat-Malureanu, J. P. Carlo, P. L. Russo, A. T. Savici, A. Aczel, G. J. MacDougall, J. A. Rodriguez, G. M. Luke, S. R. Dunsiger, A. McCollam, J. Arai, C. Pfleiderer, P. Böni, K. Yoshimura, E. Baggio-Saitovitch, M. B. Fontes, J. Larrea, Y. V. Sushko, and J. Sereni, Nat. Phys. **3**, 29 (2007).

[37] C. Pfleiderer, P. Bøni, T. Keller, U. K. Rößler, and A. Rosch, Science **316**, 1871 (2007).

[38] See, e.g., J. Spehling, Ph.D. thesis, TU Dresden, 2013.

[39] R. Khasanov, Z. Guguchia, A. Maisuradze, D. Andreica, M. Elender, A. Raselli, Z. Shermadini, T. Goko, E. Morenzoni, and A. Amato, High Pressure Res. **36**, 140 (2016).

[40] Z. Shermadini, R. Khasanov, M. Elender, G. Simutis, Z. Guguchia, K. V. Kamenev, and A. Amato, High Pressure Res. **37**, 449 (2017).